CHEMISTRY
A EUROPEAN JOURNAL

DOI: 10.1002/chem.200800374

Two-Component Hydrogels Comprising Fatty Acids and Amines: Structure, Properties, and Application as a Template for the Synthesis of Metal Nanoparticles

Hajra Basit,[a, b] Asish Pal,[a, b] Saikat Sen,[a] and Santanu Bhattacharya*[a]

Abstract: Stearic acid or eicosanoic acid mixed with di- or oligomeric amines in specific molar ratios form stable gels in water. The formation of such hydrogels depends on the hydrophobicity of the fatty acid, and also on the type of amine used. The gelation properties of these two-component systems were investigated using electron microscopy, FTIR spectroscopy, ^{1}H NMR spectroscopy, differential scanning calorimetry (DSC), and both single-crystal and cast-film X-ray diffraction. Results of FTIR spectral analysis suggest salt formation during gelation. ^{1}H NMR analysis of the gels indicates that the fatty acid chains are immobilized in the gel state and when the gel melts, these chains regain their mobility. Analysis of DSC data indicates that increase in the spacer length in the di-/oligomeric amine lowers the gel-melting temperature. Two of these gelator salts developed into crystals and structural details of such systems could be secured by single-crystal X-ray diffraction analysis. The structural information of the salts thus obtained was compared with the XRD data of the self-supporting films of those gels. Such analyses provided pertinent structural insight into the supramolecular interactions that prevail within these gelator assemblies. Analysis of the crystal structure confirmed that multilayered lamellar aggregates exist in the gel and it also showed that the three-dimensional ordering observed in the crystalline phase is retained in only one direction in the gel state. Finally, the hydrogel was used as a medium for the synthesis of silver nanoparticles. The nanoparticles were found to position themselves on the fibers and produced a long, ordered assembly of gel–nanoparticle composite.

Keywords: fatty acids · gels · nanoparticles · supramolecular chemistry · X-ray diffraction

Introduction

Low-molecular-weight organic molecules capable of immobilizing or arresting the flow of liquids are popularly termed as low-molecular-weight gelators (LMWG).[1] The solvents immobilized can be either organic or aqueous. These LMWGs assemble into various three-dimensional aggregates such as rods, long fibers, strands, tubules, or globules.[2] Many of these self-assembled aggregates provide a route to generate ordered nano- or microsized materials serving as a tool in the "bottom-up" fabrication of nano-, opto-, and electronic devices.[3] Hydrogel (gelation of water) formation is of particular interest due to its various biological applications, for example, vehicles for controlled drug release,[4] tissue engineering,[5] or topical applications.[6]

Such gelators include a wide variety of molecular structures such as long-chain hydrocarbons,[7] amino acid derivatives,[8] carbohydrate-derived systems,[9] metal complexes,[10] dendrimers,[11] and steroid derivatives.[12] It is well documented that for a molecule to behave as a gelator it should have functional units that are capable of interacting noncovalently within themselves in an intermolecular fashion. This allows self-assembly of such molecules by means of temporal associative forces such as hydrogen bonds, π–π interactions, solvatophobic interactions, dipole–dipole interactions, van der Waals forces, and so forth. Despite these generalizations, designing and developing a new gelator capable of gelating a particular solvent continues to be a challenge.

Many gelators have been discovered serendipitously, and based on the structural guidelines that rationalize their self-assembly, similar or other gelators have been designed. The development of most of such gelators generally requires

[a] H. Basit, A. Pal, S. Sen, Prof. Dr. S. Bhattacharya
Department of Organic Chemistry, Indian Institute of Science
Bangalore 560012, Karnataka (India)
Fax: (+91) 80-2360-0529
E-mail: sb@orgchem.iisc.ernet.in

[b] H. Basit, A. Pal
These authors contributed equally to this paper.

Supporting information for this article is available on the WWW under http://www.chemeurj.org/ or from the author.

multi-step and time-consuming synthesis and tedious purification procedures. An alternative, but still relatively rare, approach in achieving gelation is by mixing two or more functional units, capable of interacting with each other to first form a 'complex' that subsequently self-assembles into a supramolecular network, thereby immobilizing the solvent.

Aqueous solutions of cationic surfactants such as cetyltrimethylammonium bromide (CTAB) and others show interesting viscoelastic properties upon addition of salts such as sodium salicylate.[13a] Such additives reduced the repulsion between the cationic amphiphilic head groups, which leads to a marked increased in the viscoelasticity of the resulting mixtures and eventual formation of hydrogels.[13b] Different surfactant micelles have been examined for such gelation and this observation was found to be true for single-headed amphiphiles.[13c] The analogous double- and triple-headed cationic surfactants did not lead to a viscoelastic mass, highlighting the importance of charge balance in such processes.[13d] Another two-component gelator system was designed by Hanabusa et al. in 1993, in which interactions between barbituric acid derivatives and derivatives of pyrimidine units were responsible for gelation.[14] Later, Oda et al. described gelation of water using cationic gemini surfactants as counter ions of D- and L-tartrate.[15a] Hydrogelation was also reported with gemini bis(hexadecyldimethylammonium)propane in the presence of palmitate.[15b] Subsequently, several interesting reports of two-component gels,[16] such as a mixture of twin-tailed anionic surfactant sodium bis(2-ethylhexyl)sulfosuccinate and phenol, appeared in literature.[17] In a true two-component gelator system, one of the components is present in isotropic solution and only the addition of a second component triggers gelation.[18] However, in some cases gels are reported in which one of the two components is capable of gelating in its own right, and the addition of a second component modifies the gelation properties.[19] There is a growing interest in mixing organic acids and bases to form organic salts that promote gelation. Sodium salts of a few bile acids in water formed viscoelastic mass and these have been studied comprehensively by Terech.[20] Smith and co-workers depicted gelation using a unique dendrimer based on L-lysine or various diamines. These investigators modulated the properties of the gel by varying the ratio of the two components.[21] Salts of aromatic acids such as cinnamic acid derivatives with aliphatic amines of varying carbon length have also been found to form organogels.[22] Recently, mixtures of cationic amino acid lysine with anionic surfactants were shown to form gels in water.[23]

The above citations provide ample evidence of the promising features of the two-component approach to achieve gelation. However, most of these studies do not provide much structural insight as to how the two components interact to form the gel. Accordingly, we were instigated to advance this problem in a rather simple way. We were curious to study the interactions between simple naturally occurring fatty acids and organic di-/oligomeric amines. Is it possible to form gels using such mixtures? If so, then what are the contributions of the individual components and their functional groups in the gel assembly? Is it possible to derive any structure–property correlation between the two components?

The interactions and phase behavior of alkaline soaps and acid soaps of long-chain fatty acids in aqueous solution has been the subject of many studies[24] because of their tremendous application in the personal-care and cosmetics industry.[25] Herein, we report the gelation properties of fatty acids with several di-/oligomeric amines in water. Among various fatty acids, stearic acid and eicosanoic acid were found to gelate water only when mixed with various oligoamines. A well-defined structure–property relationship was observed both in the fatty acid as well as in the amine part. This approach is of interest due to its relative ease of preparation, convenient modulation of material properties by variation of either component, and the possibility to tune and control (engineering). Recently, there has been a tremendous upsurge in interest in exploiting gels as a possible template for the synthesis of dimensionally ordered nanomaterials.[26] Ordered assemblies of nanometer-sized particles on their own belong to an interesting class of materials that provide the exceptional potential to achieve one-, two-, and three-dimensional organizations for a wide variety of applications ranging from photonics to memory devices, magnetic nanoparticles (NPs), and single-electron microelectronic devices.[27] Herein, we have also shown that this two-component hydrogel can also be utilized as a medium for the synthesis of silver nanoparticles.

Results and Discussion

Gel formation and characterization: Fatty acids starting from a carbon-chain length of 14 were checked for hydrogelation in the presence of various di-/oligomeric amines (Scheme 1). It was observed that myristic and palmitic acid, that is, C14 and C16 acids, were soluble in the amine solution and gave a transparent, clear aqueous solution that never formed a gel, even upon prolonged ageing (Figure 1a). However, both stearic and eicosanoic acids under these conditions gave a turbid, viscoelastic mass that afforded a stable gel on standing for 15—20 min at room temperature (Figure 1c). To probe the effect of the other fatty acids, 12-hydroxy stearic acid and oleic acid were checked for gelation under these conditions. Although each gave a turbid viscoelastic fluid, they could not gelate, even after standing for a long time (Figure 1b). It is important to note that stearic and eicosanoic acids by themselves are not soluble in water, whereas all the amines are freely soluble in water. However, the mixture of the acid with gel-forming amines rendered the fatty acid soluble in water upon heating, presumably by salt formation. These gave opaque hydrogels upon slow cooling to room temperature.

Various di- and oligomeric amines were checked for gelation with stearic and eicosanoic acids (Table 1). It was observed that only primary di-/oligomeric amines were capable

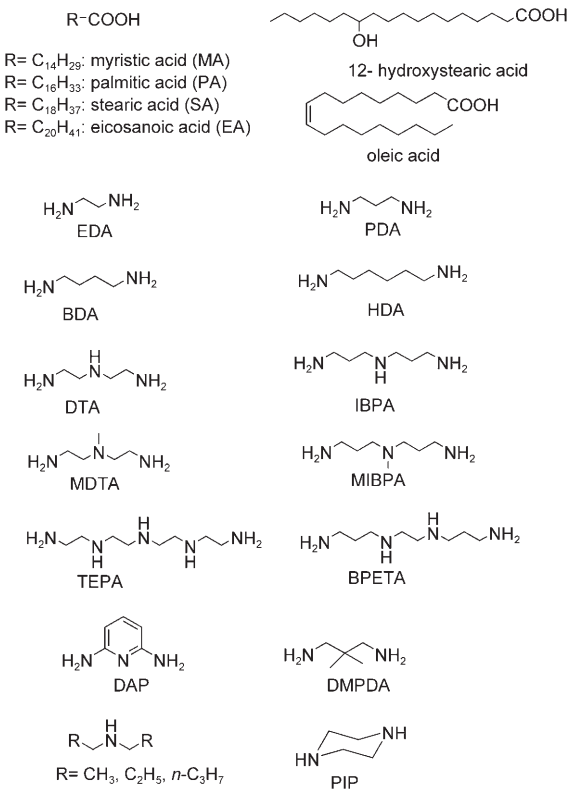

Scheme 1. Structures and abbreviations of different acids and amines checked for gelation.

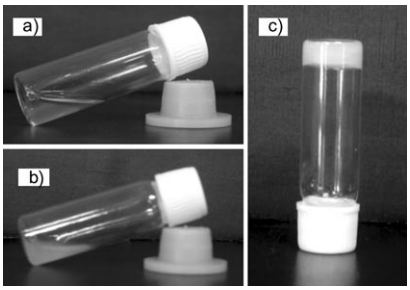

Figure 1. a) Mixture of myristic acid with IBPA, b) mixture of 12-hydroxy stearic acid with IBPA, c) typical gel of stearic acid with IBPA.

of gelation; diamines such as ethanediamine (EDA), propanediamine (PDA), and higher amines were capable of forming a gel with both stearic and eicosanoic acid. However, the gelation of eicosanoic acid was much slower than that with stearic acid. It was also observed that the ease of solubility of the acid in water was greater for higher amines (i.e., increase in the number of secondary amino groups) such as diethylenetriamine (DTA), 3,3′-iminobis(propylamine) (IBPA), *N*,*N*′-bis(3-aminopropyl)ethylenediamine (BPETA), or tetraethylenepentamine (TEPA) than the lower amines such as EDA or PDA.

Gelation of the acid was also checked with several secondary and aromatic amines to understand the role of basicity of the amine moiety. However, secondary amines such as di-

Table 1. Gelation study of various fatty acids with several amines.

Amines	Myristic acid	Palmitic acid	Stearic acid	Eicosanoic acid	12-Hydroxy stearic acid
EDA	S	S	OG	OG	S
DTA	S	S	OG	OG	S
MDTA	S	S	OG	OG	S
TEPA	S	S	TG	TG	S
PDA	S	S	OG	OG	S
IBPA	S	S	OG	OG	S
MIBPA	S	S	OG	OG	S
BPETA	S	S	TG	TG	S
DMPDA	I	I	I	I	S
piperazine	I	I	I	I	S
DAP	P	P	I	I	S

S = sol, OG = opaque gel, TG = translucent gel, I = insoluble, P = precipitate.

ethyl amine, di-*n*-propylamine, or piperazine rendered the system insoluble and thus gelation could not occur. Even the aromatic primary amine diaminopyridine (DAP) could not solubilize the acids and instead formed precipitate. Interestingly, the 2,2-dimethyl derivative of propanediamine, DMPDA, precipitated out when mixed with stearic acid and unlike its simpler analogue PDA, could not form gel. This fact could be accounted for by considering the steric hindrance or 'lock' offered by the two methyl groups at the 2-position, thereby disfavoring rotation about the bonds and making the DMPDA molecule rigid and not allowing requisite flexibility for solubilization of the acid.

Morphological characterization of the gel: The superstructures created in the hydrogel network were observed using transmission electron microscopy (TEM). The TEM images demonstrated the presence of a three-dimensional network formed by the self-assembling (SA) nanofibers of SA–DTA and SA–IBPA gels (Figure 2). The average diameters of the nanofibers were about 50–125 nm for both gels.

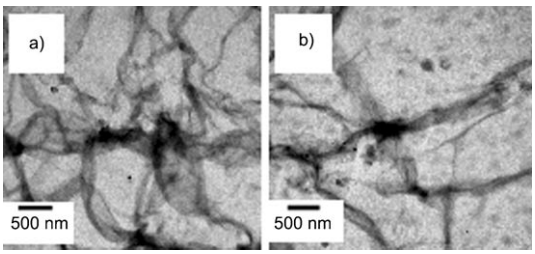

Figure 2. TEM images (stained with uranyl acetate solution) of the hydrogels of a) SA–DTA (1:3.5) and b) SA–IBPA (1:3.5).

Scanning electron micrographs (SEM) were recorded for the freeze-dried gels derived from gelators to see the detail of the gel-fiber morphology (Figure 3). All cases studied displayed typically intertwined three-dimensional networks within which the water molecules are understandably immobilized to form the gel. Gels obtained from two-component mixtures of stearic acid with either IBPA or DTA showed

structures with diameters ranging from 2 to 20 μm. SEM images of two-component gels from other amines also showed similar three-dimensional networks (see Figure S1).

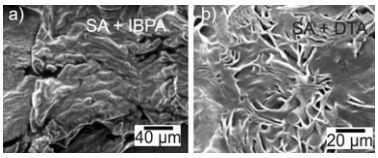

Figure 3. SEM micrographs of the hydrogels of a) SA + IBPA (1:3.5) and b) SA + DTA (1:3.5).

FTIR and HATR-FTIR studies: The formation of salt between the acid and the amine can be sensitively detected by IR spectroscopy. Because stearic acid has a characteristic carbonyl-stretching absorption band in the infrared region, this technique was utilized to determine the changes in the structural features of the molecules in the gel assembly. The symmetric stretching frequency of carboxyl carbonyl of stearic acid in solid form was 1708 cm^{-1} (see Figure S2 A). However, in the horizontal attenuated total reflection (HATR)-FTIR of the gels of SA–DTA and SA–IBPA this band lowered drastically to a value of 1650 cm^{-1}. Also, a new band that was characteristic of asymmetric carbonyl stretching appears at 1563 cm^{-1} (see Figure S2 B). These values were indicative of carboxylate salt formation.

^{1}H NMR spectra of the stearic acid–amine gels: In general, NMR techniques provide a great deal of information regarding the self-assembly process in the gel state.[17b,28] Molecules in solution (solution-phase NMR) at moderate field strengths have little preference in orientation, the tumbling samples have a nearly isotropic distribution, and average dipolar coupling goes to zero. However, in important classes of substances such as solids, liquid crystals, glasses, and gels, due to long-lived entanglements and chemical crosslinks, motions of certain segments of the molecules are strongly hindered or restricted in space and thus their dipolar interactions cannot be averaged out. The magnitude of the dipolar interaction is related to the internuclear distance as inversely proportional to its third power.[29a] When these anisotropic NMR centers present in the molecules undergo tumbling due to orientational diffusion, their NMR energy levels are modulated so that their NMR lines broaden and also shift from their usual NMR frequency values.

Thus, a correlation of the ^{1}H NMR spectra of the species in solution with that of gel provides an insight into the self-assembly process.[29b] Figure 4I shows the ^{1}H NMR spectra of a solution of stearic acid in $CDCl_3$, propanediamine (PDA) in D_2O, and the gel of SA (0.07 M)–PDA (0.24 M) in D_2O at various temperatures. At 25 °C, for the gel of stearic acid and PDA in D_2O, a significant line broadening of the proton signals of the acid was observed, to the extent that they almost disappeared. This suggests that almost all of the acid was incorporated into the gel, rendering it more or less solid-like and thus its molecular motion was restricted. This also indicates that the orientation of these chains is such that they minimize interactions with water. However, minor downfield shifts of amine protons in the gel state were observed, along with broadening of their signals (Table 2). The presence of these signals suggests the involvement of excess amines in the gel network. The signal of the water present in D_2O at 4.78 ppm also appeared broadened, indicating that the water molecules are part of the gel assembly. Upon heating the gels up to the melting temperature, recovery of the resonance lines of the acid were observed closer to the gel-melting temperature (45 °C) and there was a dramatic sharpening of these resonance lines upon complete gel melting (55 °C). Furthermore, with gradual breakdown of gel network, a minor downfield shift was observed for the amine protons (columns marked "a" and "b" in Table 2).

Similarly, the gel of SA (0.07 M)–IBPA (0.24 M) in D_2O at various temperatures showed significant line broadening of the protons of the acids and the amines at 25 °C (Figure 4II and Table 2), though upon heating to 45 °C, the resonance peaks started to become sharp. This observation was consistent with the understanding that the acid molecules experience severe mobility restrictions in a gel, and that gel melting would indirectly imply melting of the chains that are now in a state of higher mobility, thereby averaging out or minimizing the dipolar interactions between ^{1}H nuclei. This fact is well advocated by the ^{1}H NMR spectrum of a non-gel-forming system, that is, of myristic acid (MA) and PDA (Figure 4III). The mixture of myristic acid (0.07 M) and PDA (0.24 M) taken in D_2O remains only as a turbid solution and does not gelate (discussed above). Thus, the resonance lines of neither the acid nor the amines appear broadened and also no shift in the frequency of these signals is observed, indicating isotropic tumbling of the molecules in solution. It may be noted that the spectrum of the acid is recorded in $CDCl_3$ because of its insolubility in water, whereas that of the acid–amine mixture is in D_2O. Thus, a minor upfield shift of the proton signals of the acid in the gel could be attributed to the solvent effect.

Differential scanning calorimetry: Thermal stability and thermoreversibility of the gel is of interest in respect to its various applications, such as drug delivery. To gain further insights into the thermal stability of the gels of stearic acid with various amines, differential scanning calorimetric studies were performed. As the gel was heated, a peak due to transition from gel to sol was observed. When the sol was cooled, it exhibited a peak due to transition from sol to gel. Repeated heating and cooling showed similar transition behavior, indicating the thermoreversible nature of the gel assembly. In addition, the melting temperatures (T_m) for the gel to sol were found to be ≈10–12 °C higher than the gel-forming temperature (T_f) for the sol to gel transition, which is typical of many LMWG-based gels (Figure 5).[30]

An intriguing structure–property relationship between the acid and the amines was reflected in the thermal melting data of these gels. The gels from di-/oligomeric amines of

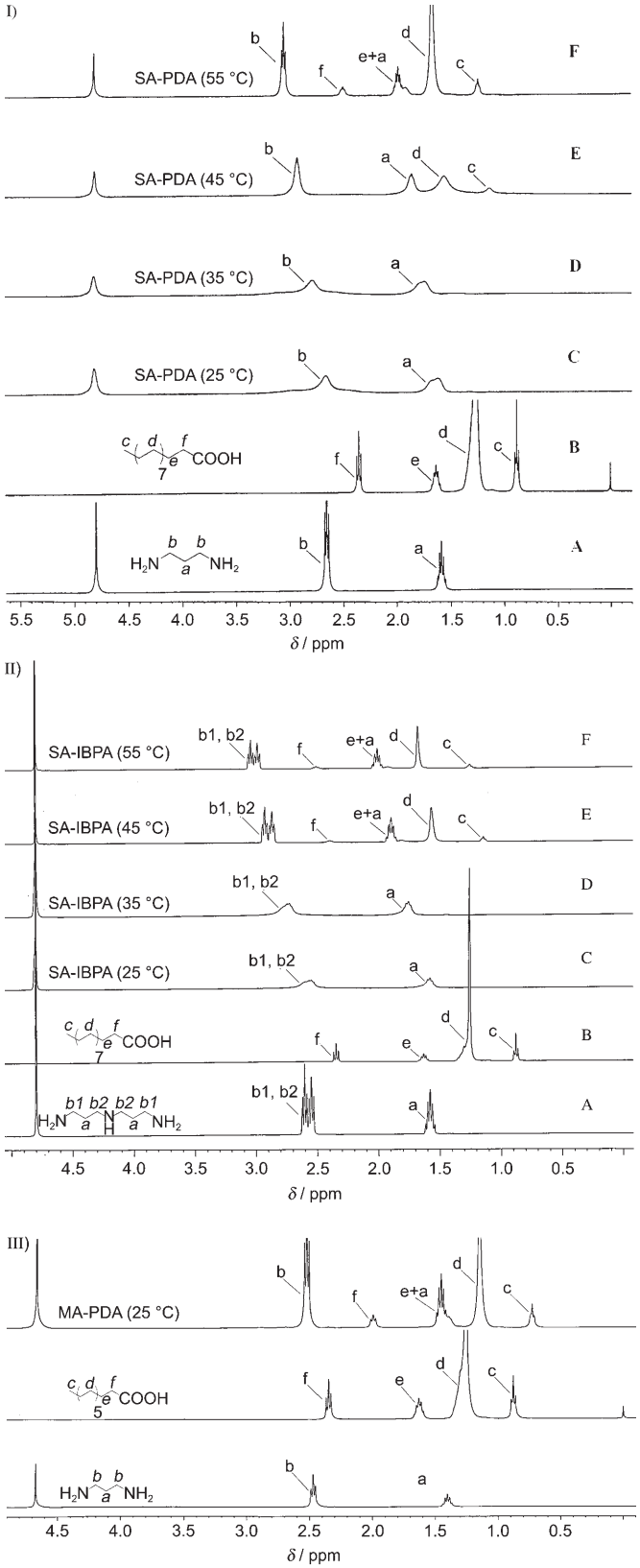

Figure 4. I) ^{1}H NMR spectra (400 MHz) of A) PDA in D_2O, B) stearic acid (SA) in $CDCl_3$. Gel of SA–PDA (1:3.5) in D_2O at C) 25 °C, D) 35 °C, E) 45 °C (gel starts to melt), F) 55 °C (entire gel has melted). Concentration of stearic acid in hydrogel is 0.07 M in each case. II) ^{1}H NMR spectra (400 MHz) of A) IBPA in D_2O, B) stearic acid (SA) in $CDCl_3$. Gels of SA–IBPA (1:3.5) in D_2O at C) 25 °C, D) 35 °C, E) 45 °C, F) 55 °C. Concentration of stearic acid in hydrogel is 0.07 M in each case. III) ^{1}H NMR spectra (400 MHz) of PDA in D_2O (bottom), myristic acid (MA) in $CDCl_3$ (middle), and a solution of MA–PDA (1:3.5) in D_2O (top). Concentration of myristic acid is 0.07 M in each case.

Table 2. Temperature shifts of diverse signals [ppm] of the hydrogels of SA in D_2O with PDA and IBPA.

	a	b
PDA (D_2O)	1.58	2.65
SA–PDA (25 °C)[a]	1.62 (br)	2.69 (br)
SA–PDA (35 °C)	1.73 (br)	2.81 (br)
SA–PDA (45 °C)	1.89 (br)	2.94 (br)
SA–PDA (55 °C)	1.96	3.03
IBPA (D_2O)	1.59	2.60, 2.55
SA–IBPA (25 °C)[b]	1.59 (br)	2.57 (br)
SA–IBPA (35 °C)	1.75 (br)	2.72 (br)
SA–IBPA (45 °C)	1.90	2.92, 2.83
SA–IBPA (55 °C)	2.05	3.03, 2.98

[a] [SA] = 0.07 M, [PDA] = 0.245 M. [b] [IBPA] = 0.245 M.

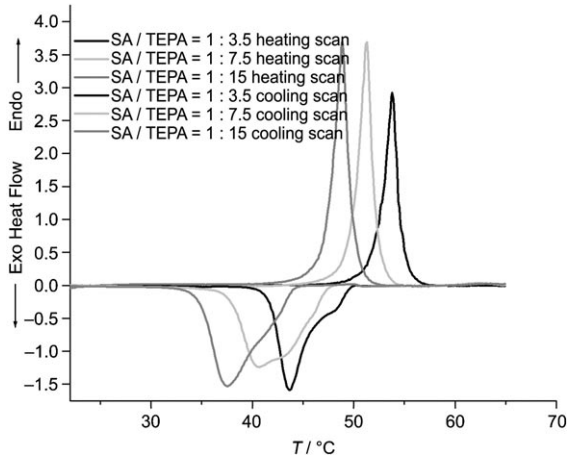

Figure 5. Representative DSC thermograms of the gel of SA and TEPA at different molar ratios of acid and amine. Concentration of stearic acid in hydrogel is 0.07 M in each case.

ethylene spacer have in general a higher melting point than the gels prepared with amines of propane spacer (Figure 6). It was also evident that increasing the chain length in the diamine moieties, that is, from ethanediamine to hexanediamine, made the gels thermally less stable (Figure 6A). This could be due to the tighter packing of the acid–amine salts by diamines of ethylene spacer than those of propylene spacer, and a further increase in chain length in the form of butanediamine and hexanediamine made the packing even weaker.

Furthermore, the increase in the number of methylene groups from EDA to PDA to BDA to HDA increased the thermal motion in the assembly and thus facilitated the gel to sol transition.

It was also ascertained form the thermal melting data (Figure 6B, C) as a function of amine/acid molar ratio that

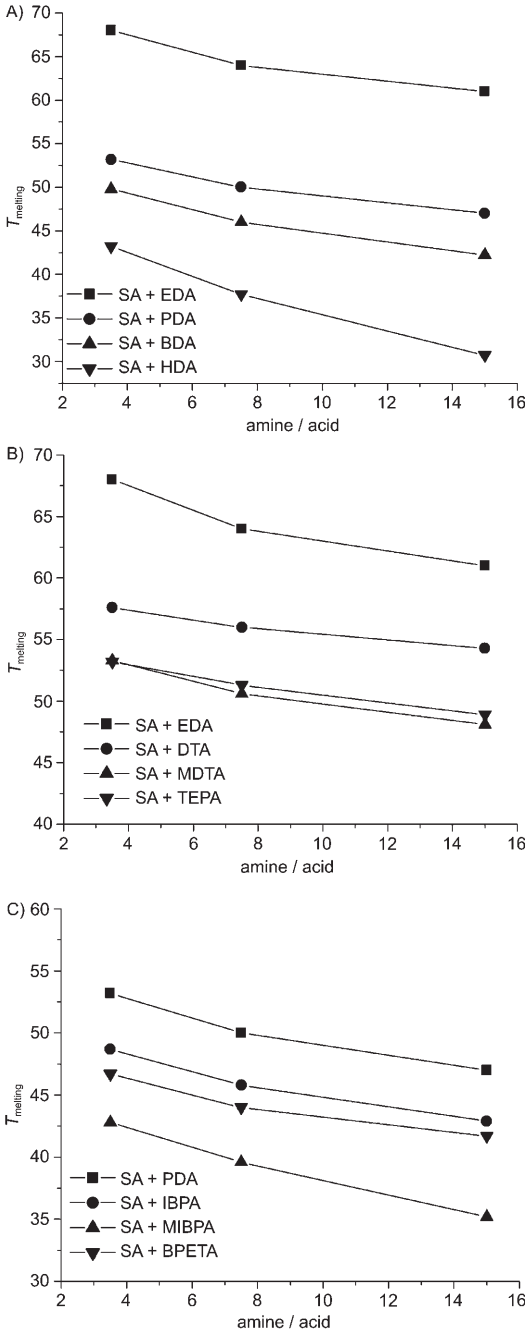

Figure 6. Plot of T_m against molar ratio of A) different diamines of varying spacer length and stearic acid, B) different oligoamines with even spacers and stearic acid, and C) different oligoamines with odd spacers and stearic acid.

in the case of triamines, that is, DTA and IBPA, the gel-melting temperature decreased drastically when the secondary amine proton was replaced by a methyl group, as in *N*-methyldiethylenetriamine (MDTA) and *N*-methyliminobis(propylamine) (MIBPA). This implies that the additional hydrogen bonding supplied by the secondary amino proton is abolished when it is replaced by the methyl group, thereby making the acid–amine assembly less resistant to thermal energy. This fact indicates the contribution of the secondary amine protons to the gel assembly. It may also be noted from the melting data of Tables S1 and S2 that upon increasing the concentration of the amine, the melting temperature of the gels was gradually lowered. During preparation of the gels it was observed that as the concentration of the amine was increased, the acid became readily soluble in the system and the gels also became slightly translucent and "loose". This indicates that at higher concentration of amine, the system becomes more "sol-like". Thus, it may be inferred that an excess concentration of amine made the mixture more hydratable by increasing the number of hydrogen-bonding sites offered by both primary and secondary amines. These excess amines presumably interfere with the hydrogen-bonded sites of the gel network making the gel network weaker. Thus, a large excess concentration of amines is an impediment to the stability of the supramolecular hydrogen-bonded gel assembly here.

Single-crystal analysis of the gelator salts: Analysis of the solid-state supramolecular assembly of a gelator molecule, if available, would provide useful insights into the intermolecular interactions that might be responsible for the gel-fiber formation.[31] Hydrogen-bonding-directed self-assembly of acid–base mixtures in the solid state is known.[32] To this end, we made several attempts to obtain single crystals of the salts SA–EDA and SA–PDA, suitable for single-crystal X-ray diffraction analysis from solutions of stearic acid and the corresponding amine mixed in a 2:1 molar ratio. However, crystallizing these salts in the presence of even small quantities of their gelating solvent proved to be a daunting task. Indeed, in the case of SA–EDA, most attempts to grow a single crystal with water, water–methanol/isopropanol, or butanol mixtures were futile, as the gelator would merely gelate water from the solvent mixture. Use of either slow-solvent evaporation or the ether-vapor-diffusion technique in solutions of SA–EDA in dry polar solvents such as methanol and isopropanol gave rather poor-defined polycrystalline aggregates. Eventually, single crystals of SA–EDA, suitable for X-ray diffraction analysis, were obtained from a solution of stearic acid and EDA in 10:2:1 chloroform/methanol/water by employing the slow-solvent-evaporation technique under ambient conditions. Though less restrictive than in case of SA–EDA, the use of water as a crystallization solvent for SA–PDA consistently led to formation of good-quality plate-like, albeit midget, crystals. One such tiny pre-grown single crystal was introduced as a nucleating agent in a solution of stearic acid and PDA in 1:4 isopropanol/water and allowed to grow by means of slow solvent evaporation for about one week under ambient dust-free conditions. The best crystal of SA–PDA from the various batches was selected for single-crystal X-ray diffraction analysis.

Crystal structure of SA–EDA: The 2:1 salt of stearic acid and ethanediamine (SA–EDA) formed typically thin plate-like crystals with an average thickness <0.02 mm. This, coupled with the absence of any strong atomic scatterers,

caused the crystals of SA–EDA to diffract quite weakly, even upon prolonged exposure to the X-ray beam. Nevertheless, after tedious attempts, satisfactory X-ray diffraction data with good intensity statistics could be collected on a $0.12 \times 0.10 \times 0.03\ mm^3$ crystal of SA–EDA (see Table S3). Subsequent structure solution and least-squares refinement on F^2 was carried out in the centro-symmetric triclinic space group $P\bar{1}$. The asymmetric unit of the crystal structure of SA–EDA was found to contain a stearate anion in a general position, and a (2-ammonioethyl)ammonium cation occupying the crystallographic inversion center at (1, 0, $^1/_2$) (Figure 7). The fully ordered cation and anion exhibited

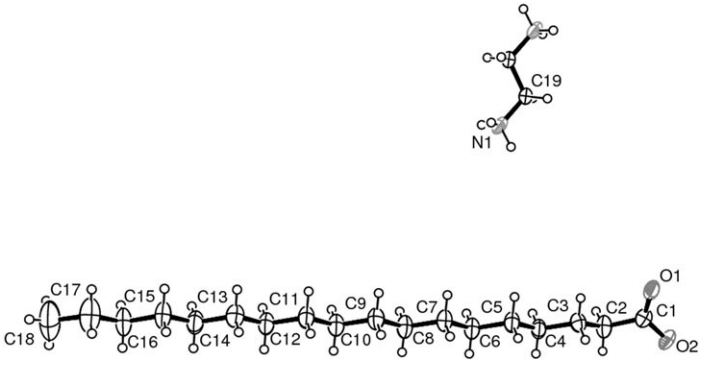

Figure 7. ORTEP diagram of the SA–EDA, with the atom numbering scheme for the asymmetric unit. Displacement ellipsoids have been drawn at 50% probability level and hydrogen atoms are shown as small spheres of arbitrary radii.

almost perfect staggering of the C–C and C–N bonds. The C17 alkyl chain of the stearate anion is inclined toward the longest crystallographic axis, the *c* axis. The two ionic components of SA–EDA are held in the crystal structure by N-H···O hydrogen bonds, with each ammonium moiety of the cation and the carboxylate group of the anion participating in three H-bonds each (Table 3). Exhibiting a near tetrahedral environment around each N atom, each cation is, therefore, linked to six stearates to form an interesting channel-like architecture, composed of a polar interior and a lipophilic exterior, around each crystallographic inversion center at (0, 1/2, 1/2). The supramolecular assembly of SA–EDA thus formed further ensures parallel stacking of the C17 alkyl chains of the stearate units in the crystal structure so as to optimize the weak van der Waals forces between the lipophilic components, not only within each channel-like architecture, but also between those translated along the *c* axis (Figure 8).

Table 3. Hydrogen-bond geometry in SA–EDA [Å, °].

D-H···A[a]	D-H	H···A	D···A	D-H···A
N1-H1A···O1^{i}	0.89	1.88	2.761 (4)	170
N1-H1B···O1^{ii}	0.89	1.80	2.682 (4)	173
N1-H1C···O2^{iii}	0.89	1.94	2.806 (5)	165

[a] Symmetry codes: i) $x+1, y-2, z$; ii) $x, y-1, z$; iii) $x, y-2, z$.

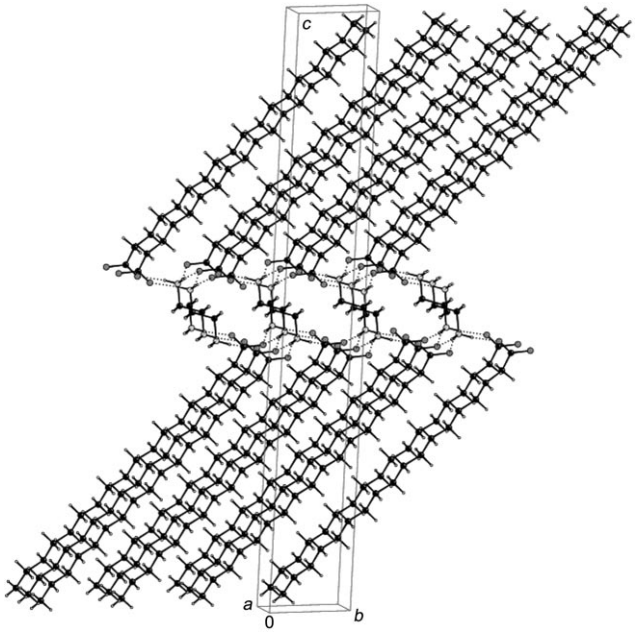

Figure 8. Molecular packing of SA–EDA showing the columnar supramolecular architectures, characterized by a lipophilic exterior and a polar interior.

Crystal structure of SA–PDA: As alluded to above, the 2:1 salt of stearic acid and propanediamine (SA–PDA) formed typically thin plate-like crystals, which like SA–EDA, diffracted quite weakly in the X-ray beam. However, unlike SA–EDA, crystals of SA–PDA were seen to deteriorate and lose their crystallinity over time, probably on account of dehydration. Thus, the data-collection strategy was optimized with respect to exposure time in order to obtain as good data completion and intensity statistics as possible (Table S3). Subsequent structure solution and least-squares refinement on F^2 was carried out in the centro-symmetric triclinic space group $P\bar{1}$. SA–PDA was found to crystallize as a dihydrate, with the asymmetric unit of the crystal structure containing two stearate anions, a (3- ammoniopropyl)-ammonium cation, and two molecules of water, all occupying general positions (Figure 9). Like SA–EDA, the fully ordered cation and anion exhibited almost perfect staggering of the C–C and C–N bonds. The C17 alkyl chains of the two symmetry-independent stearate anions are inclined towards the long crystallographic axis, the *c* axis. The two ionic components of SA–PDA are held in the crystal structure primarily by N-H···O hydrogen bonds, with each ammonium moiety of the cation participating in three H-bonds and the carboxylate group of the anion participating in four H-bonds (Table 4). Therefore, each cation is bonded to six stearates to form an interesting channel-like architecture, composed of a hydrophilic interior, encapsulating the water molecules, and a lipophilic exterior. The parallel stacking of

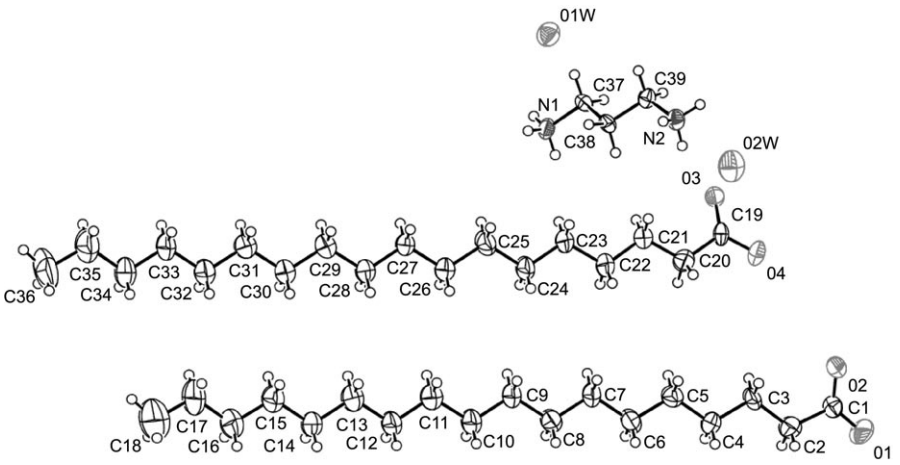

Figure 9. ORTEP diagram of the SA–PDA, with the atom numbering scheme for the asymmetric unit. Displacement ellipsoids have been drawn at 50% probability level and hydrogen atoms are shown as small spheres of arbitrary radii.

Table 4. Hydrogen-bond geometry in SA–PDA [Å, °].

D-H···A[a]	D-H	H···A	D···A	D-H···A
N1-H1A···O2^{i}	0.89	1.91	2.772 (4)	162
N1-H1B···O4^{ii}	0.89	1.92	2.811 (4)	175
N1-H1C···O1^{iii}	0.89	1.81	2.696 (4)	173
N1-H2A···O1^{iv}	0.89	1.94	2.823 (4)	173
N1-H2B···O1^{v}	0.89	1.93	2.814 (4)	172
N1-H2C···O4^{vi}	0.89	2.15	3.003 (5)	160

[a] Symmetry codes: i) $x+1, y-1, z$; ii) $-x+2, -y, -z+1$; iii) $x+2, y-1, z$; iv) $-x+2, -y+1, -z+1$; v) $x-1, y, z$; vi) $-x+1, -y+1, -z+1$.

the C17 alkyl chains of the stearate units observed in the crystal structure of SA–PDA optimizes the weak van der Waals forces between the lipophilic components, not only within each channel-like architecture, but also between those translated along the *c* axis (Figure 10).

X-ray diffraction: To envisage the supramolecular aggregation in gels and also to be able to extend a correlation of the single-crystal structure to that of the gel state, thin-film XRD patterns of the gels were recorded. The patterns for gels of both SA–EDA and SA–PDA prepared from water showed periodic reflection peaks (Figure 11), which indicates that both of these gels form an ordered lamellar organization. The long spacing or the Braggs constant (*d*) of the SA–EDA gel is observed to be 39.09 Å (Figure 11I, inset A). Interestingly, this value matches quite well with the value of long spacing value (*d*) of the crystal of SA–EDA, 39.18 Å. This spacing corresponds to the (001) plane and is the *c* axis in the crystal structure. Similarly, for the XRD of the thin film of gel of SA–PDA the *d* spacing value is 38.747 Å, (Figure 11II, inset A), whereas from the simulated XRD pattern of the single crystal of SA–PDA the long-spacing value (*d*) is 38.951 Å ((001) plane and *c* axis of the unit cell). This indicates that the symmetry along the *c* axis of the crystal structure of both SA–EDA and SA–PDA is maintained or translated in the gels of SA–EDA and SA–PDA, respectively. It is observed for both SA–EDA and SA–PDA that the higher-angle peaks in the XRD of gels and xerogels are 1/2 or 1/3 or 1/4 or higher-ratio multiples of the longest *d* spacing, that is, they correspond to the reciprocal space group (002) or (003) or (004) etc., respectively (Figure 11I and II, inset B). The peaks overlap almost exactly with their respective ones in the simulated XRD patterns of the crystals. Thus, we can conclude that the molecular packing along long spacings (*d*) in the gel structure of salts under

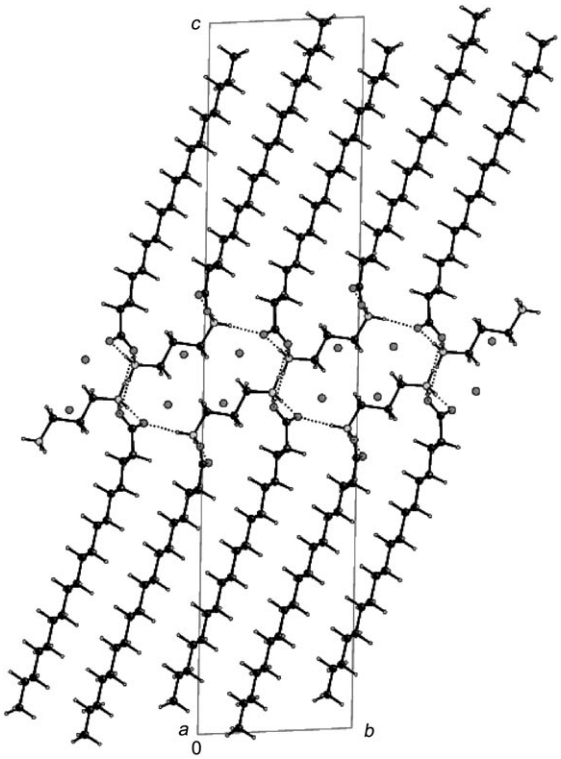

Figure 10. Molecular packing of SA–PDA showing the columnar supramolecular architectures, characterized by a lipophilic exterior and a hydrophilic interior.

study should resemble that observed along the [001] direction of their crystalline phase. As outlined below, this premise made visualization of the supramolecular assembly in the SA–diamine gels a relatively simple task. On the basis of various analyses such as FTIR, XRD, ^{1}H NMR it is clear that stearic acid and amines form salts in the gel and adopt a lamellar arrangement, in which the head group, that is, the carboxylate ions, interact with the amines and trapped water

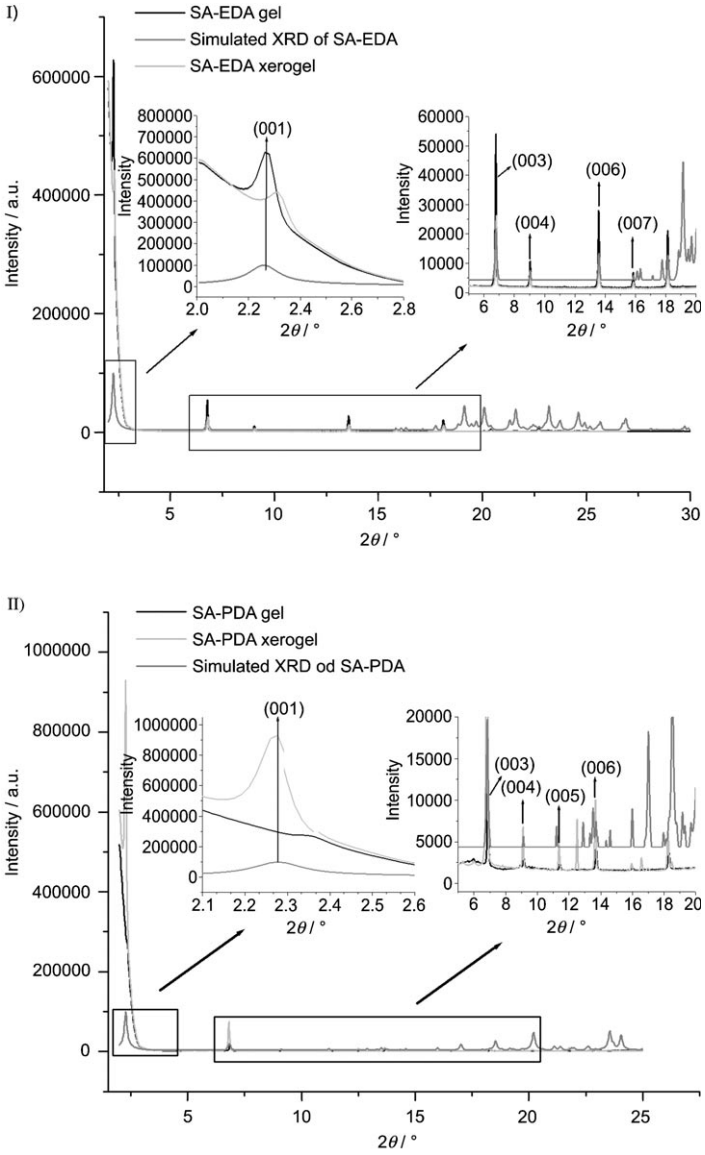

Figure 11. I) Overlay of the XRD pattern of SA–EDA gels, xerogels, and simulated XRD pattern from the crystal. Inset A depicts the magnification in the lower-angle region indicating the same longest *d* spacing for gel, xerogels, and crystal. Inset B shows the magnification in the 2θ range 5—20°. II) Overlay of the XRD pattern of SA–PDA gels, xerogels, and simulated XRD pattern from the crystal. Inset A depicts the magnification in the lower-angle region indicating the same longest *d* spacing for the gel, xerogel, and crystal. Inset B shows the magnification in the 2θ range 5—20°.

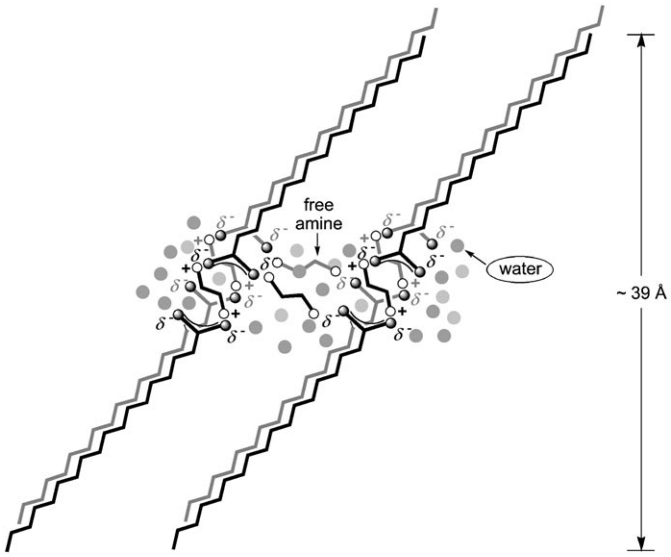

Figure 12. Proposed lamellar arrangement of the stearic acid–diamine salt in the gel assembly (SA–EDA shown here as an example).

molecules through electrostatic forces and hydrogen bonding. An appropriate model that considers all the evidence is depicted in Figure 12. Notably, unlike crystallization, gelation requires a critical excess of amine (two to four times the concentration of the acid), however, when the amine concentration is much larger than this, the gel becomes loose. Thus, it is quite likely that in the gel state, one primary amino group of one di-/oligomeric amine would be protonated while the other would remain neutral. These protonated amines remain as "tight" ion pairs with the carboxylate anions, thereby holding the network together. The unprotonated amino groups align in such a way that there is a continuous hydrophilic cavity where the water (solvent) and the excess amines associate to form a dense hydrogen-bonded network. Such an interior core should be the pocket in which several water molecules are held by interfacial tension leading to the formation of hydrogel.

Synthesis of silver nanoparticles in hydrogel: To examine whether these hydrogel networks could be utilized for the synthesis of metal nanoparticles we considered the following. Apart from the Brust method,[33] a number of other methods for synthesizing metal nanoparticles using thiol and amines have been reported.[34] Among these, carboxylate-capped metal NPs have attracted considerable attention.[35] Besides citrate-stabilized Ag colloid,[36] fatty acids/amines have also been used for synthesizing metal NPs, though these long-chain hydrophobic capping agents can form stable monodisperse metal colloids only in nonpolar solvents.[37] Recently, the synthesis of long-chain-amine-capped water-soluble NPs has also been reported.[38] Antonietti et al. exploited for the first time water-swollen gels as an medium for the synthesis of metal NPs,[39] and since then, considerable attention has been given to gel-network-templated metal NPs syntheses.[26] Because in the present gel network hydrophilic channels are present in the vicinity of carboxylate and protonated amine, it occurred to us that the gel networks could be used as a template for synthesizing an assembly of Ag colloids.

The syntheses of gel–Ag–NP composite were accomplished using a procedure described in the Experimental Section. Briefly, $AgNO_3$ was reduced using $NaBH_4$ in melted hydrosol of SA–amine, which upon cooling afforded the nanocomposites in which the Ag colloids were stabilized by the gel fibers(see Figure S3). These gel-Ag-NP compo-

sites were thermoreversible and on repeated heating–cooling the gelation behavior remained intact. The surface plasmon bands for Ag-NPs templated on the hydrogel networks of SA–IBPA and SA–BPETA are shown in Figure 13. Both the Ag–NP composite samples showed a characteristic surface plasmon band for Ag-NPs at ≈409 nm. Note that attempted Ag–NP synthesis in water using stearic acid or the amine alone in the presence of $NaBH_4$ resulted in immediate formation of a brownish precipitate. The resulting residue could not be resuspended in aqueous media.

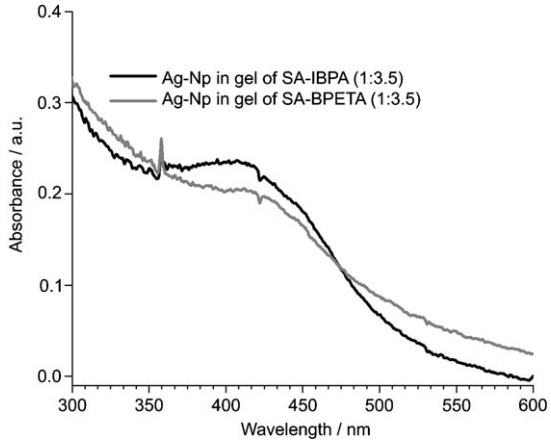

Figure 13. UV-visible absorption spectra of gel-Ag-NP composite made from SA–IBPA (1:3.5) and SA–BPETA (1:3.5) gels.

The size and the possible assembly of nanoparticles were investigated by transmission electron microscopy. The TEM images of SA–IBPA–Ag–NP composite showed the formation of spherical silver NPs that were 4–7 nm in diameter (Figure 14). Interestingly, the particles were found to be aligned along the gel fibers in a reasonably long assembly. Most of the NPs were confined to the gel fibers with lengths on the micrometer scale and diameters in the order of 40–120 nm. Because the fibers were much larger than the Ag-NPs they could act as a host on which the NPs are embedded during fiber formation. Regardless of the specific arrangements of the particles, this work clearly shows the immobilization of the NPs on the gel fibers. Thus, this two-component gel was shown to be an excellent medium for stabilizing the Ag-NPs, which emerged as a convenient method for obtaining the composite materials.

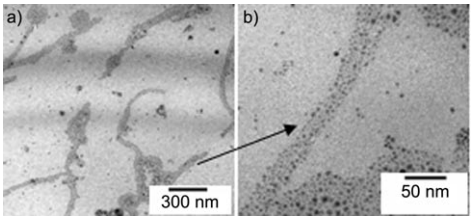

Figure 14. TEM images of gel-Ag-NP composite. a) Ag-NP synthesized in hydrogel of SA–IBPA (1:3.5). b) Magnified images of Ag-NP preferentially residing on gel fibers.

Conclusion

We have identified an extremely simple but novel water-gelation system using the principle of organic salt formation involving a fatty acid of suitable length and dimeric or oligomeric amine. The primary salt-bridging interactions between the two components involving carboxylate and ammonium ion are reflected in the FTIR spectrum. These interactions then lead to a continuous hydrogen-bonded network forming gel. The packing of the stearic acid units is such that they keep away from the water molecules due to hydrophobic effect, thus resulting in a closely or tightly entangled network, as seen from results of ^{1}H NMR spectroscopy. The fibers that form the gel yield a lamellar arrangement of interdigitated fatty acid moieties that are stabilized by weak van der Waals forces, electrostatic interactions, and hydrogen bonding. The thermal strength of the gels depends on the type of spacer present (two or three carbon atoms) in the amine moiety. In general, the additional hydrogen-bonding sites provided by the secondary amine group modulates the thermal properties of the gels. Correlation between the single-crystal structure analysis and XRD of gels makes it possible to envisage the supramolecular arrangement present in the gel state. This approach of gelation is an alternative to the extensive multi-step synthetic procedures in designing a gelator and also provides a tool or handle in modulating the properties of the gel. Furthermore, varying the molar ratio of the two components provides an additional level of control over the properties of the materials. Also, the presence of hydrophilic pockets along the fibers provided the opportunity to make new composite materials in which the assembly of nanoparticles can be controlled and grown along the fibers. Thus, this design of organic–inorganic hybrid with a high order of nanoscopic structure from readily available starting materials could be extended to developing materials with specific properties.

Experimental Section

Materials and methods: All the chemicals were procured from Aldrich and Fluka and were used without further purification. Milli-Q grade water was used for all physical measurements.

Gelation studies: In a typical gelation study experiment, a stock solution of desired concentration of the respective amine was prepared in water. Different aliquots of this stock solution were diluted with water to get amine solutions of required concentration, into each of which was added a weighed quantity of acid (solid). Each mixture was heated to 60–70 °C and bath sonicated using Transsonic T460/H for three minutes to get a homogenous solution. This solution was allowed to cool to ambient temperature gradually. The vial was then inverted. If no flow was observed with the resulting mass then it was termed a gel. Each experiment was performed in duplicate.

Transmission electron microscopy: The gels were carefully melted to sol and 10 μL of sol was drop-coated onto a carbon-coated copper grid (200

mesh size) and allowed to dry at RT. Then, 10 μL of 0.1% uranyl acetate aqueous solution was drop-coated onto the sample and allowed to stand for 24 h. The samples were further dried under vacuum for 2 h. For TEM of gel-Ag-NP composite, 10 μL of melted sol was drop-coated onto a carbon-coated copper grid and allowed to dry at RT for 24 h and was further dried under vacuum for 2 h. TEM images were taken at an accelerating voltage of 100 kV using a TECNAI F30.

Scanning electron microscopy: Representative gel was carefully melted to sol and 50 μL of the sol was transferred onto brass stubs and allowed to form gel on the stubs. The sample was freeze-dried, then coated with 10-nm thick gold films using a BAL-TEC SSD-500 sputter coater instrument. Finally, the morphology of the gels was imaged on a FEI-Quanta 200 SEM operated at 5 kV.

Attenuated total reflection FTIR studies: The FTIR spectra were recorded in H_2O by using a Perkin–Elmer GX FTIR spectrophotometer with a horizontal attenuated total reflection (HATR) detector. An amount (20 μL) of the gel was carefully spread on a Zn–Se plate to form a uniform layer. The infrared spectra were recorded by collecting ten scans at a resolution of 4 cm^{-1}. The spectra of the gels were processed by subtraction of the water spectrum from the spectra of the samples. The IR spectral analysis was carried out using a spectrum version 3.02 (Perkin–Elmer) software as well as Origin 6.1 software.

NMR measurements: ^1H NMR spectra of gels of stearic acid with various oligoamines were recorded by using an AMX 400 MHz (Bruker) spectrometer using D_2O as the solvent. The concentration of stearic acid was 0.07 M and that of the amine was 0.245 M.

Differential scanning calorimetry: Gel samples of stearic acid with different amines were prepared as mentioned above and their thermotropic behaviors were investigated by high-sensitivity differential scanning calorimetry using a CSC-4100 model multicell differential scanning calorimeter (Calorimetric Sciences Corporation, Utah, USA). Gels were heated to sol and 0.4 mL of clear sols was taken into DSC ampoules. The ampoules were sealed and the gels were allowed to set overnight at ambient conditions. Measurements were taken within the temperature range of 10–80 °C at a scan rate of 20 °C h^{-1}. At least two consecutive heating and cooling cycles were performed. Baseline thermograms were obtained by using the same amount of water in the respective DSC cells. The thermograms for the gel were obtained by subtracting the respective baseline thermogram from the sample thermogram using 'CpCalc' software provided by the manufacturer. From the plot of excess heat capacity against temperature, the gel-to-sol transition temperature (T_m) was obtained.

Single-crystal structure analysis: Single-crystal X-ray diffraction data were collected by using a Bruker AXS SMART APEX CCD diffractometer at 291 K. The X-ray generator was operated at 50 kV and 35 mA using $Mo_{K\alpha}$ radiation. The data were collected with a ω scan width of 0.3°. A total of 606 frames per set were collected using SMART[40a] in four different settings of ϕ (0, 90, 180, 270°) keeping the sample-to-detector distance at 6.062 cm and the 2θ value fixed at −28°. The data were reduced by SAINTPLUS;[40b] an empirical absorption correction was applied using the package SADABS,[41] and XPREP[40] was used to determine the space group. The crystal structures were solved by direct methods using SIR92[42] and refined by full-matrix least-squares methods using SHELXL97.[43] Molecular and packing diagrams were generated using ORTEP32, CAMERON, and MERCURY, respectively. The geometric calculations were performed by using PARST[44] and PLATON.[45] All the hydrogen atoms were placed in geometrically idealized positions and allowed to ride on their parent atoms. Details of data collection and refinement are given in the Supporting Information.

X-ray diffraction studies: Various samples of gels (20 mg mL^{-1}) were individually and carefully placed on a pre-cleaned glass slide and left to air dry for 8 h in a dust-free environment. This yielded the self-supported cast films on which measurements were performed using a Phillips X-ray diffractometer. The X-ray beam generated by using a Cu anode at the wavelength of the $Cu_{K\alpha}$ beam at 1.5418 Å, was directed towards the film edge and scanning was done from a 2θ value of 2–30°. Data were analyzed and interpreted in terms of higher-order reflections.

Silver nanoparticles synthesis: In a typical preparation, 0.5 mL of hydrogel made from SA–IBPA (1:3.5) was taken into a vial and heated to 50 °C to convert it to a sol. Then, 20 μL of 0.05 M aqueous $AgNO_3$ solution was added to the mixture and magnetically stirred for 2 min. To this, 5 μL of aqueous solution of $NaBH_4$ (0.5 mg mL^{-1}) was added which caused a yellow color within ≈1 min indicating formation of silver nanoparticles in the medium. On cooling to RT, the resulting mixture solidified into a hydrogel nanocomposite comprising Ag-NP. The hybrid material was characterized by UV/Vis spectroscopy (Surface Plasmon) and TEM.

Acknowledgements

We thank Professor K. Venkatesan and Professor G. Mehta for useful discussions. We are grateful to the Institute Nanoscience Initiative (INI) for TEM and SEM, DST India for the CCD facility, and the Centre for NMR research at IISc, Bangalore. This work was supported by funding from FMC-India.

[1] M. George, R. G. Weiss, *Acc. Chem. Res.* **2006**, *39*, 489–497.
[2] L. A. Estroff, A. D. Hamilton, *Chem. Rev.* **2004**, *104*, 1201–1217.
[3] a) J. J. Storhoff, A. A. Lazarides, R. C. Mucic, C. A. Mirkin, R. L. Letsinger, G. C. Schatz, *J. Am. Chem. Soc.* **2000**, *122*, 4640–4650; b) Y. Negishi, Y. Takasugi, S. Sato, H. Yao, K. Kimura, T. Tsukuda, *J. Am. Chem. Soc.* **2004**, *126*, 6518–6519; c) M. Llusar, C. Sanchez, *Chem. Mater.* **2008**, *20*, 782–820.
[4] a) B. Jeong, S. W. Kimand, Y. H. Bae, *Adv. Drug Delivery Rev.* **2002**, *54*, 37–51; b) B. Jeong, Y. H. Bae, D. S. Lee, S. W. Kim, *Nature* **1997**, *388*, 860–862; c) B. Xing, C. W. Yu, K. H. Chow, P. L. Ho, D. Fu, B. Xu, *J. Am. Chem. Soc.* **2002**, *124*, 14846–14847; d) J. C. Tiller, *Angew. Chem.* **2003**, *115*, 3180–3183; *Angew. Chem. Int. Ed.* **2003**, *42*, 3072–3075; e) A. M. Bieser, J. C. Tiller, *Chem. Commun.* **2005**, 3942–3944; f) P. K. Vemula, J. Li, G. John, *J. Am. Chem. Soc.* **2006**, *128*, 8932–8938.
[5] K. Y. Lee, D. J. Mooney, *Chem. Rev.* **2001**, *101*, 1869–1879.
[6] Z. Yang, G. Liang, M. Ma, A. S. Abbah, W. W. Luc, B. Xu, *Chem. Commun.* **2007**, 843–845.
[7] D. J. Abdallah, R. G. Weiss, *Langmuir* **2000**, *16*, 352–355.
[8] a) S. Bhattacharya, S. N. G. Acharya, A. R. Raju, *Chem. Commun.* **1996**, 2101–2102; b) S. Bhattacharya, S. N. G. Acharya, *Chem. Mater.* **1999**, *11*, 3121–3132; c) S. Bhattacharya, Y. Krishnan-Ghosh, *Chem. Commun.* **2001**, 185–186; d) M. Suzuki, T. Sato, H. Shirai, K. Hanabusa, *Chem. Commun.* **2006**, 377–379; e) K. G. Ragunathan, S. Bhattacharya, *Chem. Phys. Lipids*, **1995**, *77*, 13–23.
[9] a) R. J. H. Hafkamp, M. C. Feiters, R. J. M. Nolte, *J. Org. Chem.* **1999**, *64*, 412–426; b) A. Srivastava, S. Ghorai, A. Bhattacharjya, S. Bhattacharya, *J. Org. Chem.* **2005**, *70*, 6574–6582; c) S. Bhattacharya, S. N. G. Acharya, *Chem. Mater.* **1999**, *11*, 3504–3511.
[10] K. Kuroiwa, T. Shibata, A. Takada, N. Nemoto, N. Kimizuka, *J. Am. Chem. Soc.* **2004**, *126*, 2016–2021.
[11] W. D. Jang, D. L. Jiang, T. Aida, *J. Am. Chem. Soc.* **2000**, *122*, 3232–3233.
[12] a) C. Geiger, M. Stanesau, L. Chen, D. G. Whitten, *Langmuir* **1999**, *15*, 2241–2245; b) N. M. Sangeetha, U. Maitra, *Chem. Soc. Rev.* **2005**, *34*, 821–836.
[13] a) C. Manohar, U. R. K. Rao, B. S. Valaulikar, R. M. Iyer, *J. Chem. Soc. Chem. Commun.* **1986**, 379–380; b) T. Shikata, H. Hirata, T. Kotaka, *Langmuir* **1989**, *5*, 398–405; c) J. Haldar, V. K. Aswal, P. S. Goyal, S. Bhattacharya, *Angew. Chem.* **2001**, *113*, 1278–1282; *Angew. Chem. Int. Ed.* **2001**, *40*, 1228–1232; d) J. Haldar, V. K. Aswal, P. S. Goyal, S. Bhattacharya, *J. Colloid Interface Sci.* **2005**, *282*, 156–161.
[14] K. Hanabusa, T. Miki, Y. Taguchi, T. Koyama, H. Shirai, *J. Chem. Soc. Chem. Commun.* **1993**, 1382–1384.
[15] a) R. Oda, I. Huc, S. J. Candau, *Angew. Chem.* **1998**, *110*, 2835–2838; *Angew. Chem. Int. Ed.* **1998**, *37*, 2689–2691; b) S. Bhattacharya, S. De, *Langmuir* **1999**, *15*, 3400–3410.

[16] a) K. Inoue, Y. Ono, Y. Kanakiyo, I. T. Ishi, K. Yoshihara, S. Shinkai, *J. Org. Chem.* **1999**, *64*, 2933–2937; b) U. Maitra, P. V. Kumar, N. Chandra, L. J. D'Souza, M. D. Prasanna, A. R. Raju, *Chem. Commun.* **1999**, 595–596; c) A. R. Hirst, D. K. Smith, *Chem. Eur. J.* **2005**, *11*, 5496–5508.

[17] a) X. Xu, M. Ayyagari, M. Tata, V. T. John, G. L. McPherson, *J. Phys. Chem.* **1993**, *97*, 11350–11353; b) M. Tata, V. T. John, Y. Y. Waguespack, G. L. McPherson, *J. Am. Chem. Soc.* **1994**, *116*, 9464–9470; c) B. A. Simmons, C. E. Taylor, F. A. Landis, V. T. John, G. L. McPherson, D. K. Schwartz, R. Moore, *J. Am. Chem. Soc.* **2001**, *123*, 2414–2421.

[18] Y. Yu, D. Nakamura, K. Deboyace, A. W. Neisius, L. B. McGown, *J. Phys. Chem. A* **2008**, *112*, 1130–1134.

[19] S. W. Jeong, S. Shinkai, *Nanotechnology* **1997**, *8*, 179–185.

[20] a) P. Terech, W. G. Smith, R. G. Weiss, *J. Chem. Soc. Faraday Trans.* **1996**, *92*, 3157–3162; b) P. Terech, B. Jean, F. Ne, *Adv. Mater.* **2006**, *18*, 1571–1574.

[21] a) K. S. Partridge, D. K. Smith, G. M. Dykes, P. T. McGrail, *Chem. Commun.* **2001**, 319–320; b) A. R. Hirst, D. K. Smith, M. C. Feiters, H. P. M. Geurts, A. C. Wright, *J. Am. Chem. Soc.* **2003**, *125*, 9010–9011.

[22] a) D. R. Trivedi, A. Ballabh, P. Dastidar, B. Ganguly, *Chem. Eur. J.* **2004**, *10*, 5311–5322; b) D. R. Trivedi, P. Dastidar, *Chem. Mater.* **2006**, *18*, 1470–1478.

[23] Y. I. Gonzalez, E. W. Kaler, *Langmuir* **2005**, *21*, 7191–7199.

[24] a) M. Heppenstall-Butler, M. F. Butler, *Langmuir* **2003**, *19*, 10061–10072; b) S. Zhu, M. Heppenstall-Butler, M. F. Butler, P. D. A. Pudney, D. Ferdinando, K. J. Mutch, *J. Phys. Chem. A* **2005**, *109*, 11753–11761; c) S. Zhu, P. D. A. Pudney, M. Heppenstall-Butler, M. F. Butler, D. Ferdinando, M. Kirkland, *J. Phys. Chem. A* **2007**, *111*, 1016–1024.

[25] a) B. Idson, *Cosmet. Toiletries* **1991**, *106*, 43–51; b) G. M. Eccleston, *Colloids Surf. A* **1997**, *123*, 169–182.

[26] a) M. Kimura, S. Kobayashi, T. Kuroda, K, Hanabusa, H. Shirai, *Adv. Mater.* **2004**, *16*, 335–337; b) K. J. C. van Bommel, A. Friggeri, S. Shinkai, *Angew. Chem.* **2003**, *115*, 1010–1030; *Angew. Chem. Int. Ed.* **2003**, *42*, 980–999; c) C. S. Love, V. Chechik, D. K. Smith, K. Wilson, I. Ashworth, C. Brennan, *Chem. Commun.* **2005**, 1971–1973; d) S. Ray, A. K. Das, A. Banerjee, *Chem. Commun.* **2006**, 2816–2818; e) P. K. Vemula, G. John, *Chem. Commun.* **2006**, 2218–2220; f) P. K. Vemula, U. Aslam, V. A. Mallia, G. John, *Chem. Mater.* **2007**, *19*, 138–140; g) S. Bhattacharya, A. Srivastava, A. Pal, *Angew. Chem.* **2006**, *118*, 3000–3003; *Angew. Chem. Int. Ed.* **2006**, *45*, 2934–2937; h) A. Pal, B. S. Chhikara, A. Govindaraj, S. Bhattacharya, C. N. R. Rao, *J. Mater. Chem.* **2008**, *18*, 2593–2600.

[27] a) Z. Y. Zhong, B. Gates, Y. N. Xia, D. Qin, *Langmuir* **2000**, *16*, 10369–10375; b) M. J. Zahn, *J. Nanopart. Res.* **2001**, 3, 73–78; c) J. Shi, S. Gider, K. Babcock, D. D. Awschalom, *Science* **1996**, *271*, 937–941.

[28] a) B. Escuder, M. Llusar, J. F. Miravet, *J. Org. Chem.* **2006**, *71*, 7747–7752; b) J. H. Jung, S. Shinkai, T. Shimizu, *Chem. Eur. J.* **2002**, *8*, 2684–2690.

[29] a) T. M. Duncan, C. Dybowski, *Surf. Sci. Rep.* **1981**, *1*, 157–250; b) D. C. Duncan, D. G. Whitten, *Langmuir* **2000**, *16*, 6445–6452.

[30] a) M. Moniruzzaman, P. R. Sundararajan, *Langmuir* **2005**, *21*, 3802–3807; b) A. Pal, Y. K. Ghosh, S. Bhattacharya, *Tetrahedron* **2007**, *63*, 7334–7348; c) S. Bhattacharya, A. Pal, *J. Phys. Chem. B* **2008**, *112*, 4918–4927.

[31] D. J. Abdallah, R. G. Weiss, *Adv. Mater.* **2000**, *12*, 1237–1247.

[32] a) S. Bhattacharya, P. Dastidar, T. N. G. Row, *Chem. Mater.* **1994**, *6*, 531–537; b) R. Kadirvelraj, A. M. Umarji, W. T. Robinson, S. Bhattacharya, T. N. G. Row, *Chem. Mater.* **1996**, *8*, 2313–2323.

[33] a) M. Brust, M. Walker, D. Bethell, D. J. Schiffrin, R. Whyman, *J. Chem. Soc. Chem. Commun.* **1994**, 801–802; b) M. Brust, J. Fink, D. Bethell, D. J. Schiffrin, C. J. Keily, *J. Chem. Soc. Chem. Commun.* **1995**, 1655–1656.

[34] a) C. K. Yee, R. Jordon, A, Ulman, H. White, A. King, M. Rafailovich, J. Sokolov, *Langmuir* **1999**, *15*, 3486–3491; b) F. Tian, K. J. Klabunde, *New J. Chem.* **1998**, *22*, 1275–1283; c) R. C. Hedden, B. J. Bauer, A. P. Smith, F. Grohn, E. J. Amis, *Polymer* **2002**, *43*, 5473–5481; d) F. Grohn, B. J. Bauer, Y. A. Akpalu, C. L. Jackson, E. J. Amis, *Macromolecules* **2000**, *33*, 6042–6050.

[35] a) W. Wang, X. Chen, S. Efrima, *J. Phys. Chem. A* **1999**, *103*, 7238–7246; b) M. Yamamoto, Y. Kashiwagi, M. Nakamoto, *Langmuir* **2006**, *22*, 8581–8586.

[36] a) P. C. Lee, D. Meisel, *J. Phys. Chem.* **1982**, *86*, 3391–3395; b) T. Yamamoto, Y. Wada, T. Sahata, H. Mori, M. Goto, S. Hibino, S. Yanageda, *Chem. Lett.* **2004**, *33*, 158–159.

[37] a) D. V. Leff, L. Brandt, J. R. Heath, **1996**, *12*, 4723–4730; b) L. O. Brown, J. E. Hutchison, *J. Am. Chem. Soc.* **1999**, *121*, 882–883; c) P. Selvakannan, S. Mandal, R. Pasricha, S. D. Adyantaya, M. Sastry, *Chem. Commun.* **2002**, 1334–1335.

[38] M. Aslam, L. Fu, M. Su, K. Vijayamohanam, V. P. Dravid, *J. Mater. Chem.* **2004**, *14*, 1795–1797.

[39] a) M. Antonietti, F. Grohn, J. Hartmann, L. Bronstein, *Angew. Chem.* **1997**, *109*, 2170–2173; *Angew. Chem. Int. Ed. Engl.* **1997**, *36*, 2080–2083; b) M. Antonietti, C. Goltner, *Angew. Chem.* **1997**, *109*, 944–964; *Angew. Chem. Int. Ed. Engl.* **1997**, *36*, 911–928.

[40] a) SMART (V6.028), Bruker AXS Inc., Madison, WI, USA, **1998**; b) SAINT (V6.028), Bruker AXS Inc., Madison, Wisconsin, USA, **1998**.

[41] G. M. Sheldrick, SADABS, University of Göttingen, Göttingen, Germany, **1996**.

[42] A. Altomare, G. Cascarano, C. Giacovazzo, A. Guagliardi, *J. Appl. Crystallogr.* **1993**, *26*, 343–350.

[43] G. M. Sheldrick, SHELXL97, University of Göttingen, Göttingen, Germany, **1997**.

[44] M. Nardelli, *J. Appl. Crystallogr.* **1995**, *28*, 659–660.

[45] A. L. Spek, *Acta Crystallogr. Sect. A* **1990**, *46*, C34.

Received: March 2, 2008
Published online: June 9, 2008

